Major findings in the second year of the project were in the following areas

1. Mesoscale model simulations, verification and sensitivity to modeling of radar reflectivity

2. Evaluating the data assimilation approach using MCMC with 1D cloud resolving model

1. Mesoscale model simulations, verification and sensitivity to modeling of radar reflectivity

The verification of WRF-ARW high resolution forecasts were performed for two IHOP events. The selected events occurred on June the 13th and June the 16th of 2002. The June 13th event was associated with a stationary/cold frontal boundary and characterized by elevated convection. At the simulation initial time, 00 UTC, multiple convective cells existed in the vicinity of Oklahoma northern border. These convective cells quickly organized into a squall line that moved north-west to south-east over the state of Oklahoma. The June 16th 2002 event was also initialized at 00 UTC. At the initial time the event was characterized by well defined meso-scale convective system (MCS) in southern KS and northern OK. The MCS developed from the merger of three smaller systems couple of hours earlier.

Simulations of the two events were performed over six hour periods, using 2-km horizontal grid spacing and 53 vertical levels and three different microphysics schemes. The three microphysics included Lin, WSM6 and Schultz. The forecast was transformed into equivalent of 3D radar reflectivity fields using "Kessler" and "RAMS" reflectivity models (described briefly in the major activities). Simulations with the more sophisticated SynPolRad model were not completed by the time of this report due to computational difficulties. This model code is very inefficient as currently implemented and would need to be optimized before it could be effectively applied to large data sets such as those from the high resolution simulations by WRF-ARW model. The current results with the high resolution simulations in the radar reflectivity space include 6 model realizations at each verification time, corresponding to the three different microphysics schemes and the two reflectivity calculation options.

For each case the observation-based LAPS analysis was produced, using the same spatial and temporal resolutions as the numerical model simulations. For this purpose all available observations including both 2D and 3D radar data reflectivity, radial velocities, other in-situ and remotely sensed data were used. The model runs used LAPS diabatic analysis as initial

conditions. The forecast verification includes comparison between the model synthetic reflectivity and the equivalent from the LAPS analysis using different skill scores.

Firstly, the sensitivity of skill scores to the two different synthetic reflectivity calculations was evaluated. The results for different reflectivity thresholds are presented in Figures 1 and 2 on the example of two microphysical parameterizations and for the case of June 13. In the case of Lin microphysics RAMS calculation of reflectivity is characterized by larger bias (ratio between number of observed and forecasted points) for all three different thresholds (20, 30 and 40 dBZ). Also, bias values increased with an increase in the reflectivity threshold (Fig. 1). Despite difference in bias, the two different approaches resulted in almost identical equitable threat score (ETS) values (Fig. 2). The same analysis using the Schultz microphysics shows similar results in terms of sensitivity of the diagnostics to the reflectivity model (Figs.1 and 2).

The skill measures calculated by using only the Kessler approach for three different microphysics and for the same thresholds are shown in Figures 3 and 4. It can be seen that changing the microphysics resulted in a notable difference in bias (fig. 3). The Lin scheme was frequently characterized with the highest bias, while opposite was true for the Schultz microphysics. All model simulations had comparable skill for all thresholds (Fig. 4). As expected the skill in all model solutions decreased with lead time. Overall, for June the 13th 2002 event Lin microphysics solution resulted in bias larger than other solutions for almost all times and for all thresholds. This was especially true when compared to model solution using the Schultz microphysics.

Figure 5 shows a west-east cross section of simulated reflectivity for the two schemes and the two different reflectivity calculation approaches. The overlaid contours represent the hydrometeor type and content. The fact that RAMS radar reflectivity calculation approach resulted in notably larger bias compared to the Kessler approach for Lin microphysics (Figs. 5a and b) pointed toward a Lin microphysics's characteristic, large graupel production (Jankov et al. 2009). Namely, the RAMS approach weights each ice component (snow, cloud ice and graupel) separately and graupel being a larger particle size is weighted more heavily than others. Given the Lin microphysics' tendency to largely overestimate presence of graupel, the RAMS approach resulted in much larger bias compared with the Kessler approach (Figs. 5a and b). In contrast, for Schultz microphysics, which is characterized by very limited graupel production (Jankov et al.

2009), different approaches in reflectivity calculation did not impact the results much (Figs. 5c and d).

Similar analyses were performed for June the 16th 2002 event. Bias calculation for the Lin and the Schultz schemes for lower thresholds show much less sensitivity to the choice of synthetic reflectivity calculation (Fig. 6). For 40dBZ threshold RAMS option was characterized by higher bias at all times compared to the Kessler option. Also, higher threshold comparison pointed toward higher bias for Schultz scheme which was opposite from findings for the June the 13th 2002 event. However, the ETS values for the two approaches were comparable for all times and all thresholds (not shown). A similar trend in bias and ETS values was observed when various microphysical schemes were compared (Fig. 7). For this event the large differences in bias were not detected among schemes at lower thresholds. For a 40 dBZ threshold the WSM6 solution is characterized by highest bias at all times, followed by Schultz and Lin. ETS values were comparable for all solutions at all times and for all thresholds.

Lastly, the contour frequency height diagrams were evaluated for the model and LAPS analysis and compared. These diagrams form bases for computing the cost function that would be used in the assimilation of reflectivity and that would represent systematic errors in vertical distribution of hydrometeor mass by the microphysical processes. Figure 8 illustrated the reflectivity-height histograms for simulation using the Lin microphysics for two reflectivity calculation approaches (Figs 8a and b) and simulation using the Schultz microphysics with the Kessler calculation approach (Fig. 8c) for the first three forecast hours. Once again, it can be seen that the RAMS calculation approach puts more weight and higher reflectivity on ice particles, especially larger ones, such us graupel. Comparison of the two different microphysics (Lin and Schultz) using the same Kessler reflectivity calculation approach, points toward larger frequency of occurrence at higher levels for the Lin scheme simulation as opposed to the Schultz simulation. Also, for this event, the frequency of occurrence seem to be larger for the Lin simulation at all heights and for all ranges of reflectivity intensity. This indicates larger presence of graupel in the case of Lin microphysics but also potentially explaining very limited trailing stratiform region in the case of the simulation using Schultz microphysics (Figs. 8b and c).

Similarly, Figure 9 shows all three model solutions for the first and the third forecast hours for June the 16th 2002 event. It can be seen that for this event the Lin solution was characterized by lower frequency of occurrence at higher and mid levels and 20-40 dBZ

reflectivity range. This agrees well with previously discussed bias and ETS analysis. Also, WSM6 solution was very comparable to the one using Schultz microphysics.

In summary,. the analysis of the two convective events indicate, not surprisingly, that the numerical model at the resolution of 2 km does not handle well events characterized by non-organized convection (single convective cells). Also, in this case as the convection got organized different microphysics performed differently (e. g. Lin was more active than other microphysics, particularly in terms of ice production). On the other hand, for the event in which the convection was well organized at the model's initial time, various model solutions ended up with comparable results. Solution using the Schultz microphysics failed to simulate trailing stratiform region, while in the case of the Lin microphysics solution the stratiform region was overestimated. At the same time all model options resulted in a very similar solution for the well developed convective line. Animations of 6 and 3-hr simulated reflectivity and the corresponding analysis with 15 min. interval for June the 13th 2002 and June the 16th 2002 events, respectively can be found at the following location: http://laps.noaa.gov/nxgn/. The file names are 13frames700_20020616_lin_kess.gif and 21frames_20020613_lin_kess.gif. These results suggests that when the phase errors are small, the different microphysical schemes exhibit compatible systematic errors, but not exactly the same. Correcting of such errors should be feasible by the data approach that is under development in the current study.

The major funding from the current WRF-ARW model validation with respect to the assimilation of the radar reflectivity observations, is that the systematic errors in vertical distribution and intensity of reflectivity, which would be used to define the cost function for improving the microphysics results and the associated precipitation forecast, are equally or more sensitive to the reflectivity model used than to the choice of microphysics parameterization. This result implies that the errors in the observation operator could dominate the background errors in the assimilation and suggests that better than relatively simple empirically-based reflectivity model should be used. One such model is the SynPolRad that is still not properly tested in the current study due to the computational inefficiency. Alternatively, the simpler model simulations may be optimized for different microphysical schemes. This could be achieved by off-line estimation of the weighting factors in the simpler model using the results of

SynPolRad or equivalent model as the reference solution. Both the computational efficiency of SimPolRad and optimization of the simpler reflectivity model will be pursued in near future.

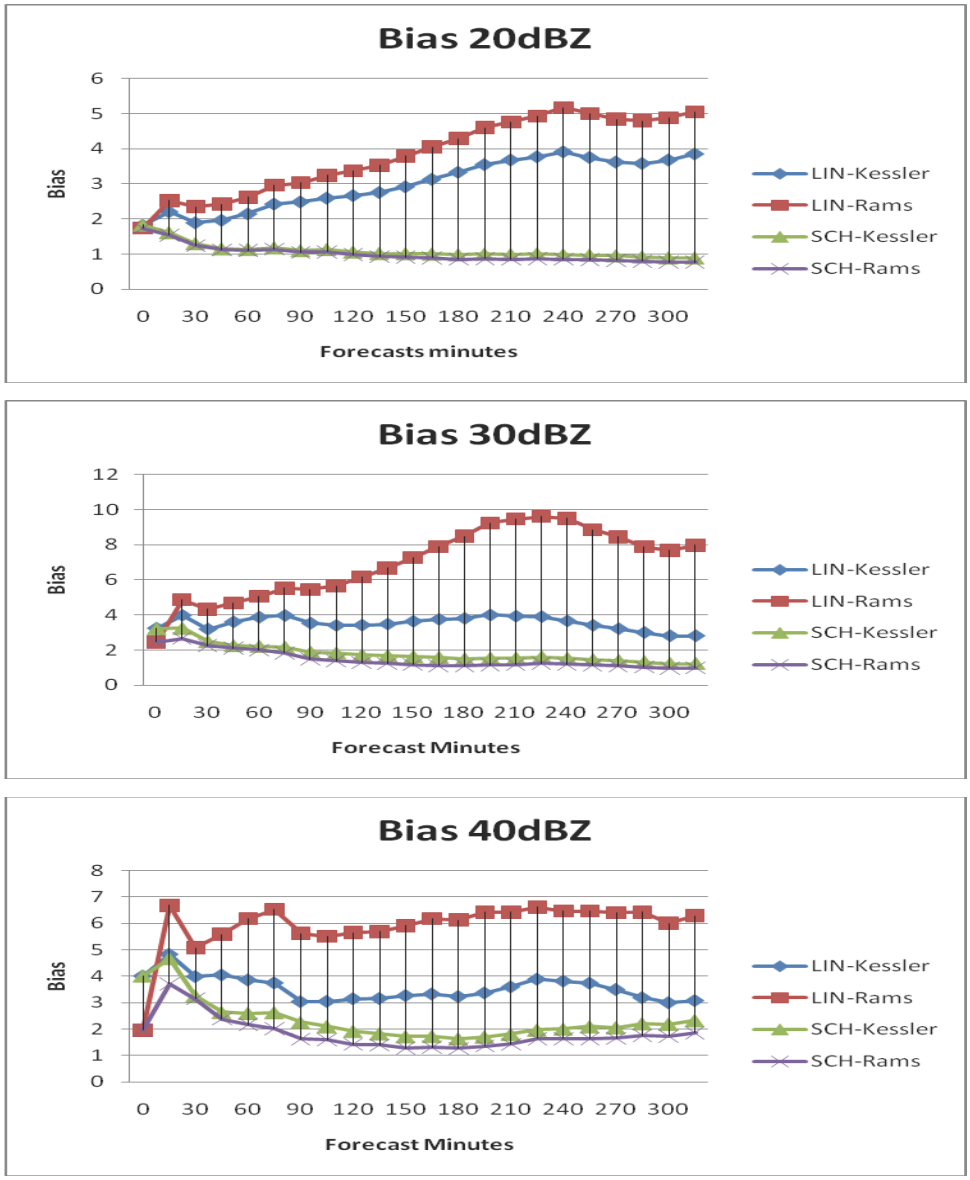

Figure 1. Bias values caluclated for the Lin and Schultz microphysics, for two different refklectivity calculation approaches (Kessler and RAMS) for three reflectivity thersholds and for simulation of June the 13th 2002 event.

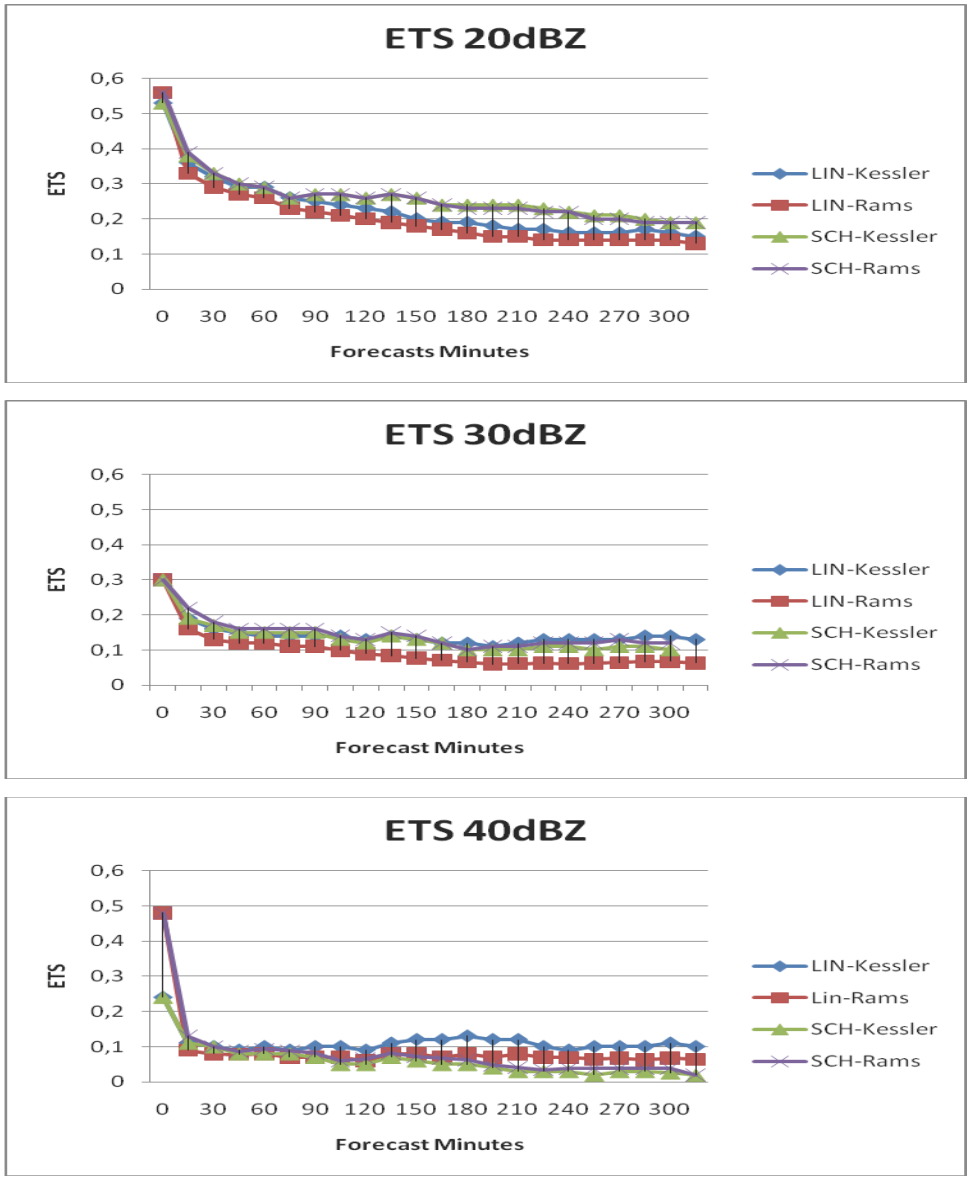

Figure 2. The same as in Fig. 1, except for ETS.

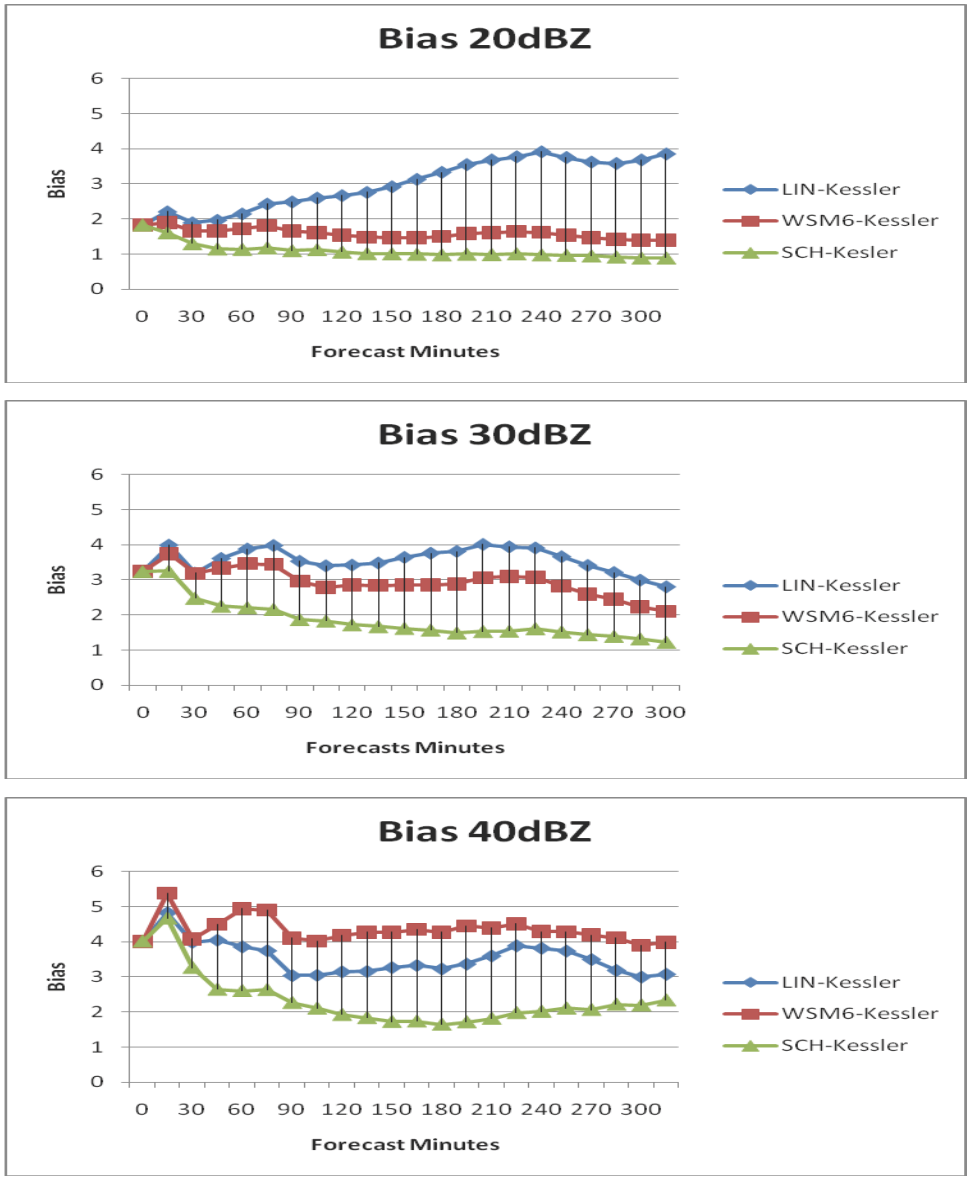

Figure 3. As in Fig.1 except for three different microphysics.

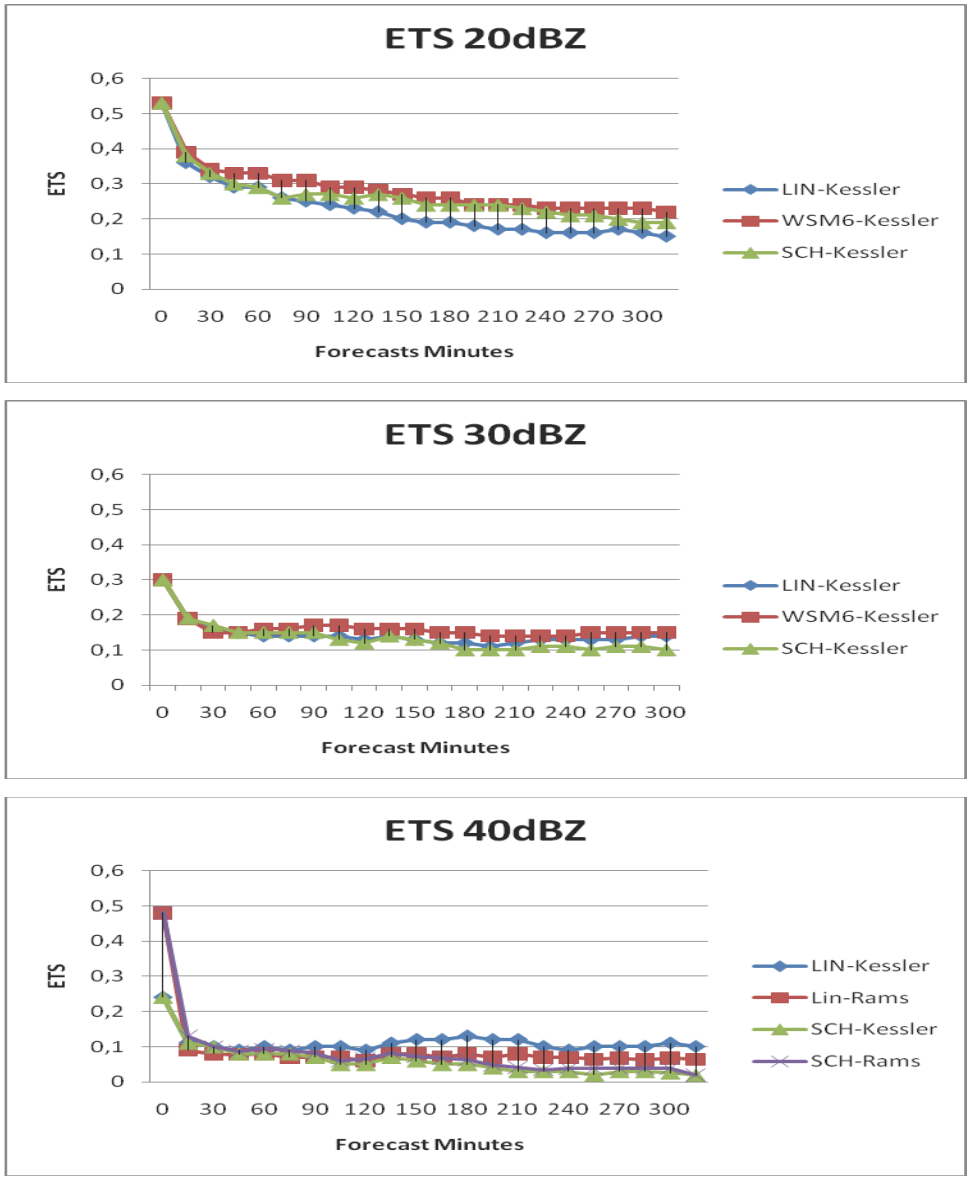

Figure 4. As in Fig. 2 except for three different microphysics.

a) b)

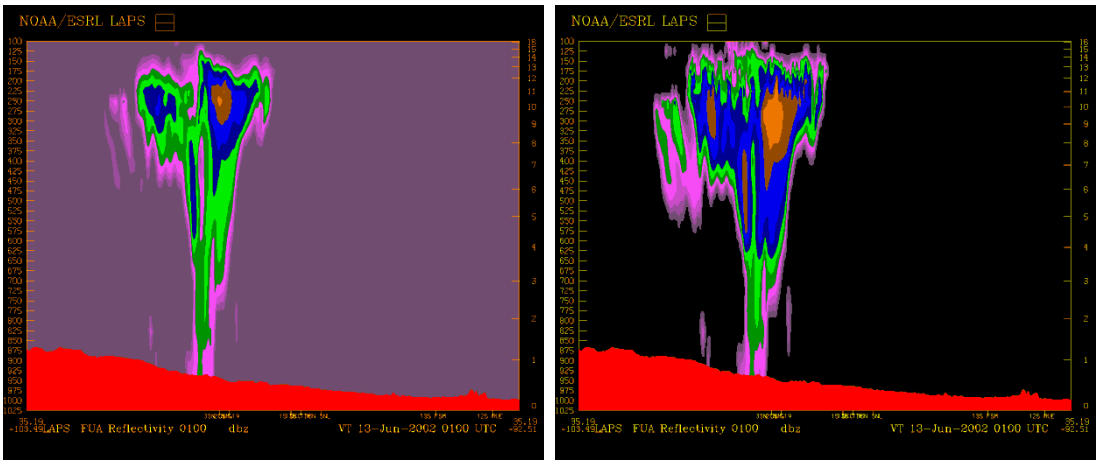

c) d)

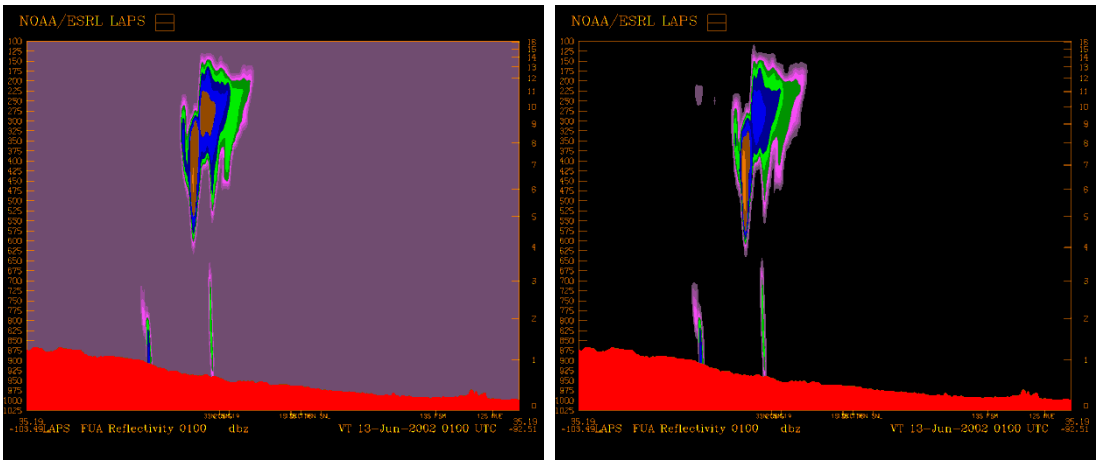

Figure 5. West-East crosssection through the middle of the integration domain of simulated reflectivity by a) Lin microphysics using Kessler, b) Lin microphysics using RAMS, c) Schultz microphysics using Kessler, and d) Schultz microphysics using RAMS reflectivity calculation for the first forecast hour of June the 13th 2002 simulation at 01 UTC.

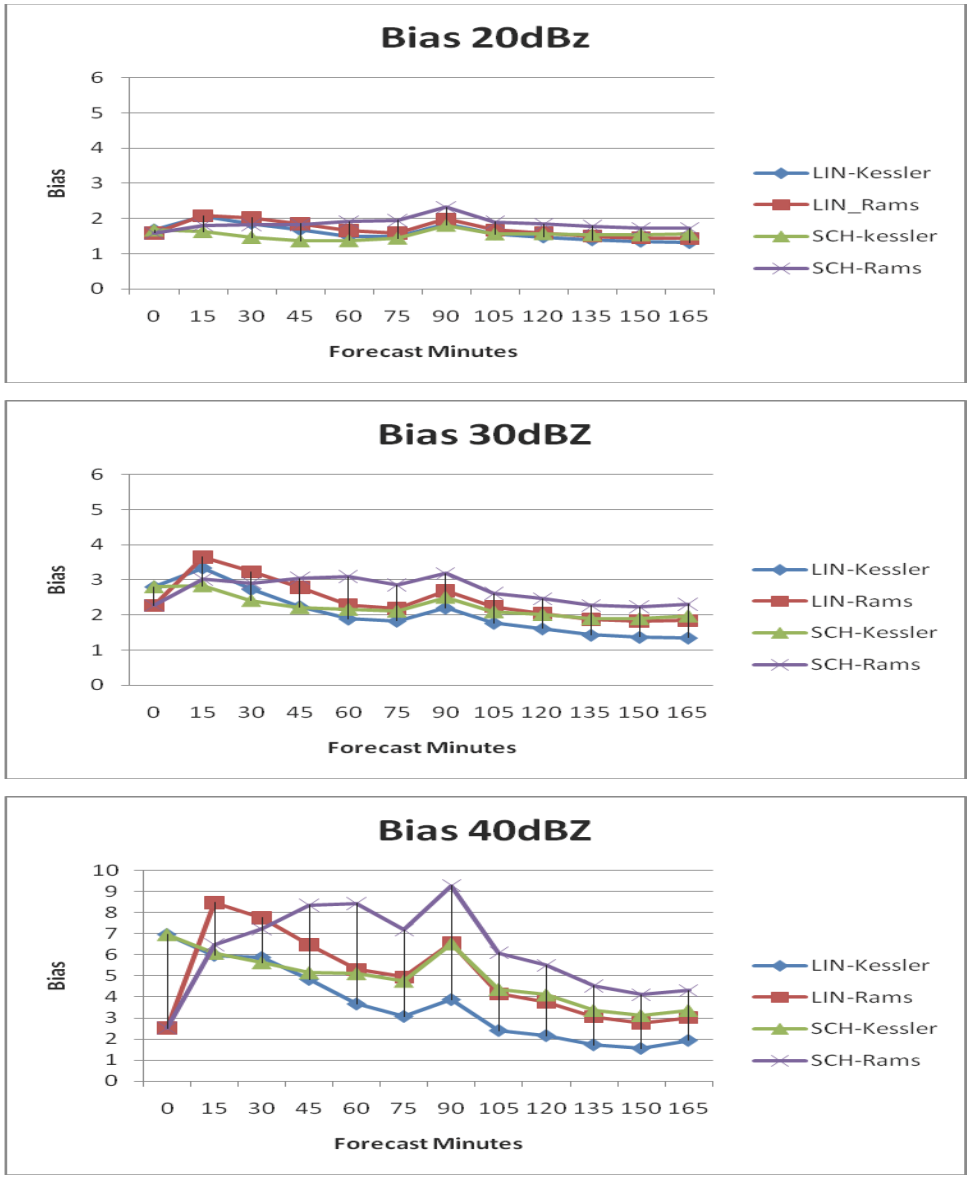

Figure 6. As in Fig.1, except for June the 16th 2002 event.

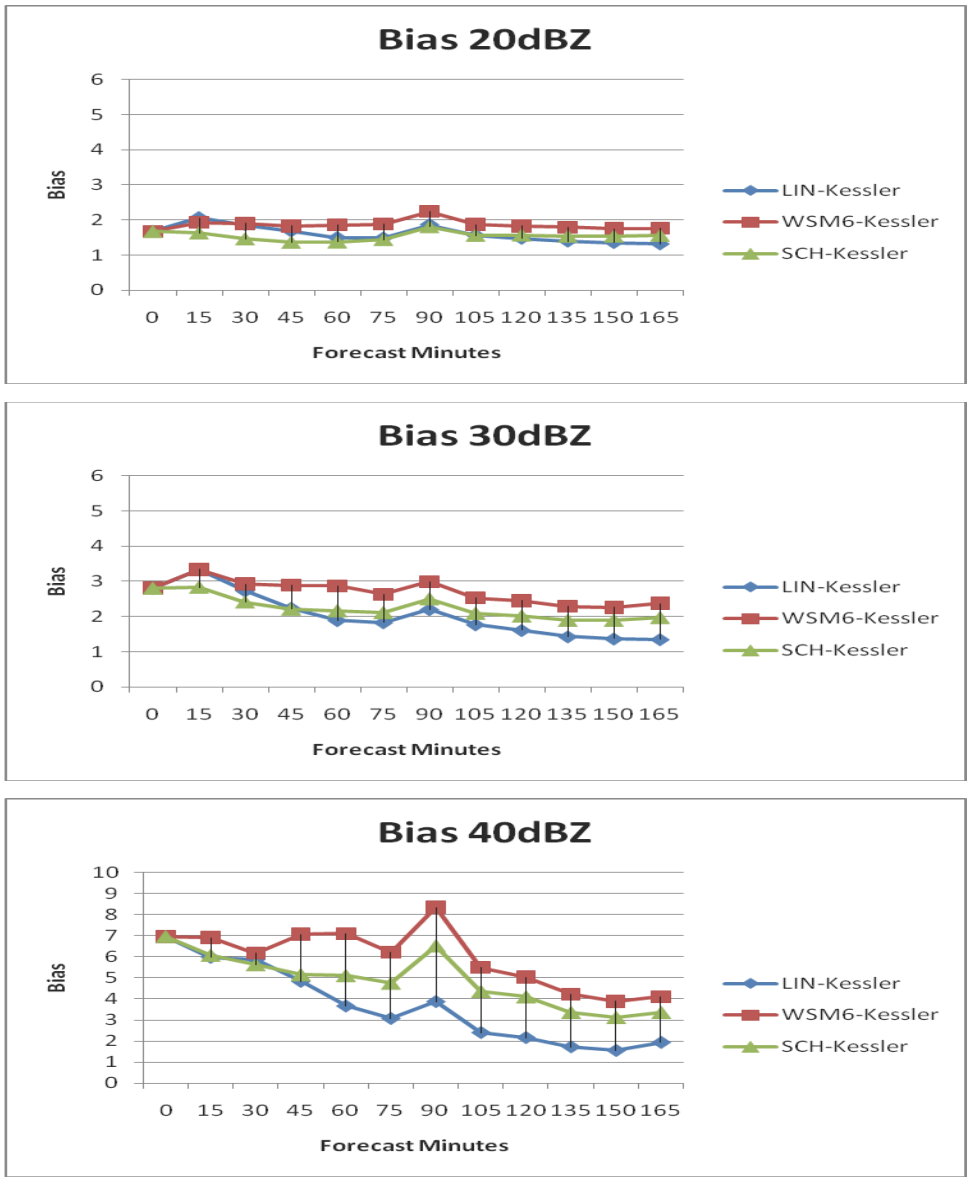

Figure 7. As in Fig. 2, except for June the 16th 2002 event.

a) Lin-RAMS

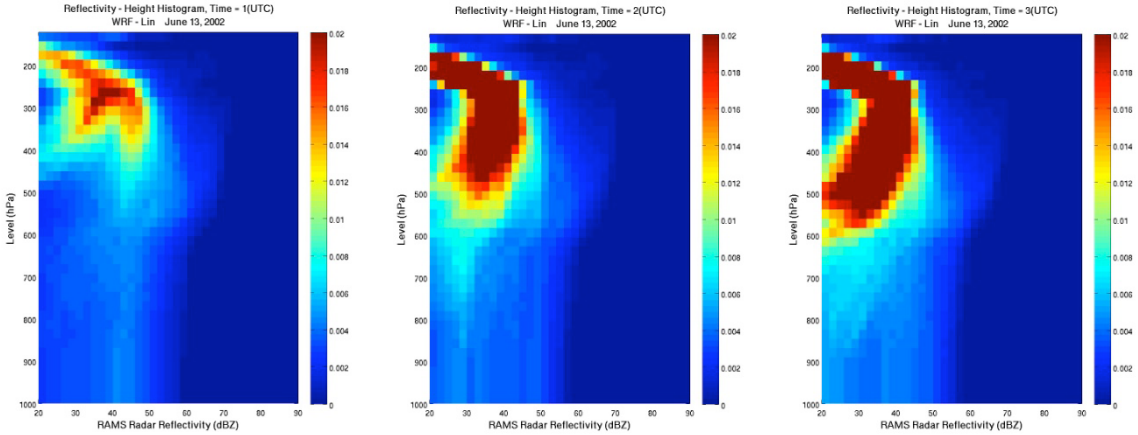

b) Lin-Kessler

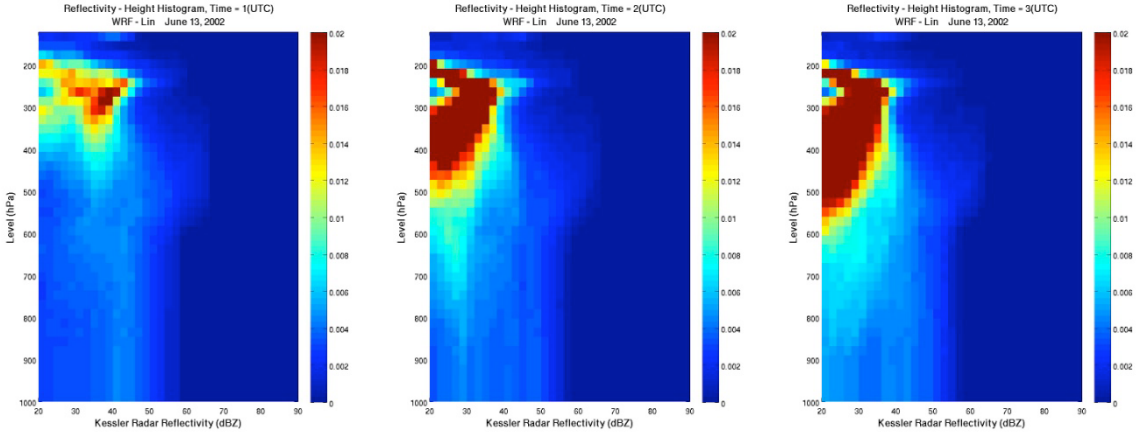

c) Schultz-Kessler

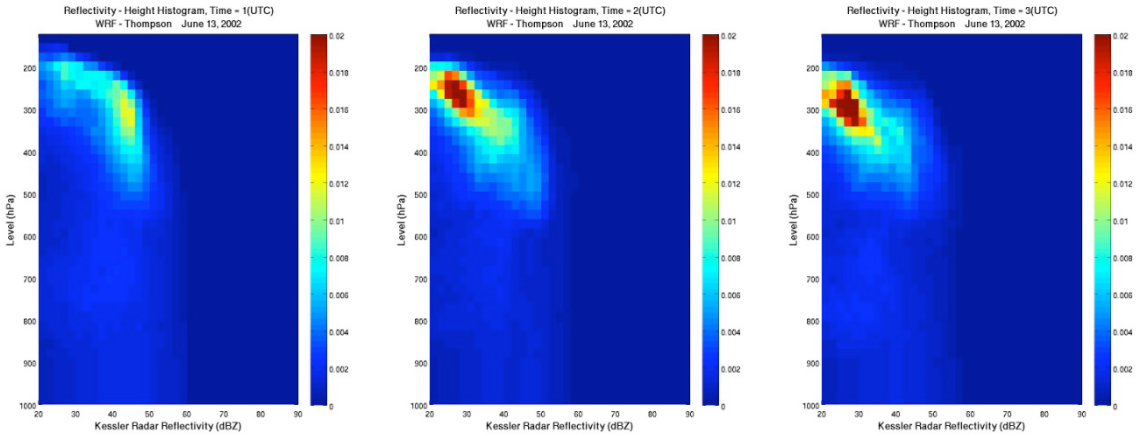

Figure 8. reflectivity-height histograms for a) Lin-RAMS, b) Lin-Kessler, and c) Schultz-Kessler for the first three forecast hours for June the 13th 2002 event.

a) Lin –Kessler

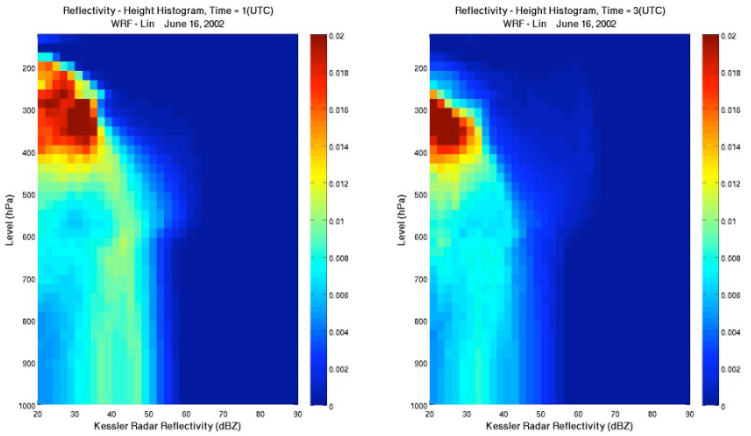

b) Schultz-Kessler

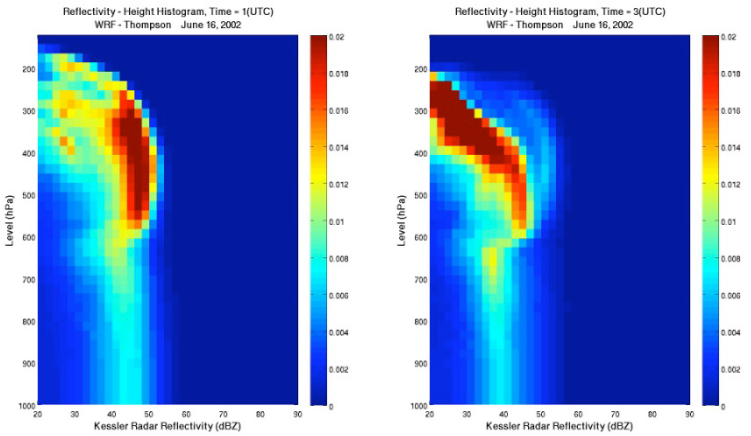

c) WSM6-Kessler

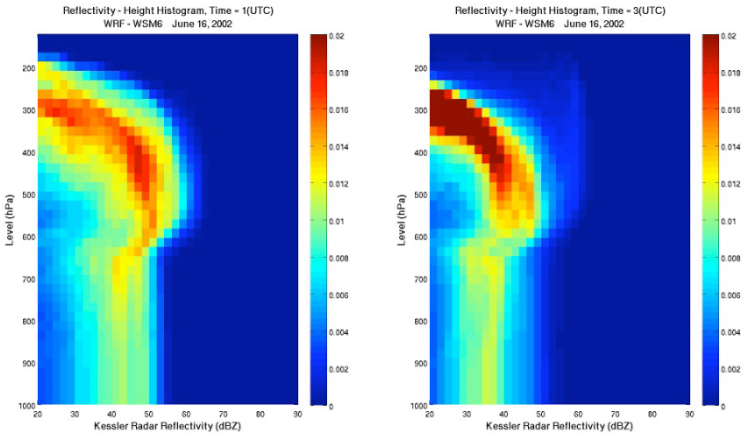

Figure 9. Reflectivity-Height histograms for the three model solutions a) Lin, b)Schultz and c) WSM6 for June the 16th 2002 event and for the 1st and the 3rd forecast hours.

2. Evaluating the data assimilation approach using MCMC with 1D cloud resolving model

As explained in the section on major activities we have implemented a 1D lagrangian cloud resolving model with MCMC (Markov Chain Monte Carlo) data assimilation algorithm (Posselt and Vukicevic, 2010) in order to evaluate properties of the radar reflectivity data assimilation problem with respect to the parameterized microphysical processes in terms of favorable conditions that would render the data assimilation problem better constrained and the solutions more accurate when using the data assimilation technique such as 4DVAR (or EnKF, for that matter). A progression of the nonlinear data assimilation problem toward well constrained formulation under varying conditions in the model and observations could be investigated thoroughly only by analysis of the full posterior pdf solutions as shown in Posselt and Vukicevic (2010). Motivated by this approach, the new activity in the project in the second year involved implementation of the 1D model and MCMC algorithm at UM by graduate student van Lier-Walqui and diagnostic analysis of the microphysical processes in the model and simulation of the reflectivity from this model solutions.

The 1D lagrangian cloud model and the MCMC algorithm are described in detail in Posselt and Vukicevic (2010). Only brief summary is presented here. The model is designed to emulate the changes in environment experienced by an atmospheric column as it moves through a cloud system following the mean flow. The vertical profiles of temperature and moisture are fixed and the model is driven by specified time-varying vertical profiles of vertical motion and water vapor tendency. Advection is only allowed to operate on cloud liquid and ice condensate, and only in the vertical direction. By varying the vertical profiles of temperature, moisture, vertical motion, and water vapor forcing, the model can be adapted to simulate the flow through a range of different cloud systems. Since organized deep convection produces the bulk of the warm season precipitation globally, (and over the Great Plains in USA) and has been shown to be highly sensitive to changes in cloud microphysical parameters, an idealized representation of squall line type convection is simulated by the model. The added benefit to examination of squall-line type convection is that it contains two discrete cloud morphologies; convective, in which precipitation is primarily generated by the collision-coalescence (warm rain) process, and stratiform, in which the melting of snow and graupel play a key role. The model is run with 60 vertical layers with constant 250 meter vertical grid spacing and a 5 second timestep, and the radiative transfer,

surface flux, and microphysical parameterizations are all identical to those used in the the NASA Goddard Cumulus Ensemble Model (Tao and Simpson 1993, Tao et al. 2003, Lang et al. 2007). Time series of rain from the model solution over 60 min is shown in Figs. 10 (equivalent to Figure 2a in Posselt and Vukicevic). It can be seen that the model produces realistic time-evolution of a squall-line with the convective phase followed by the stratiform phase.

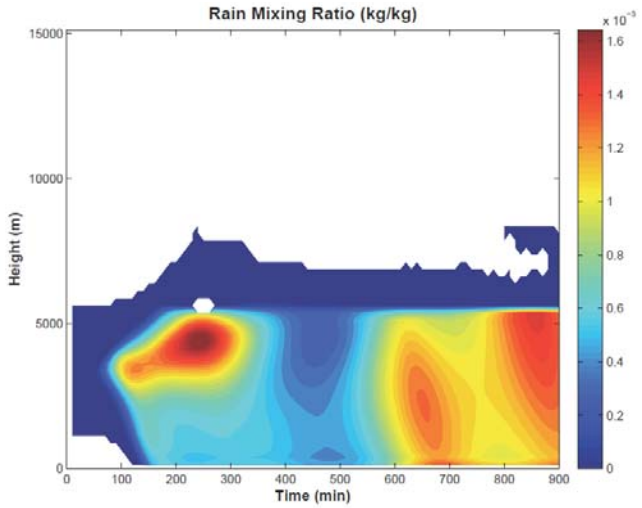

Figure 10. 1D lagrangian model simulation of time evolution of vertically distributed rain mixing ratio (kg/kg)

The current results using the 1D lagrangian cloud model are preliminary. The results include an initial analysis of the model performance in the microphysical fields and illustration of the diagnostics that would be used in further analysis and data assimilation with the MCMC system. The work leading to the current results was performed over only relatively short period of time during Jan-March 2010, because both the graduate student and PI Vukicevic have been focusing majority of efforts prior to that time to activities related to transitioning to the new appointments.

a) Simulation of reflectivity and polarimetric differential reflectivity using SimPolRad

The radar observation model SimPolRad has been implemented with the 1D modeling system. This observation model enables simulations of radar measurements that are more explicitly sensitive to properties of the hydrometeors including the type, size and shape, than the standard radar measurements. The simulated standard reflectivity and the associated differential reflectivity are

shown in Figure 11. For this simulation the model solution for all liquid and ice hydrometeors are used (not shown).

(a)

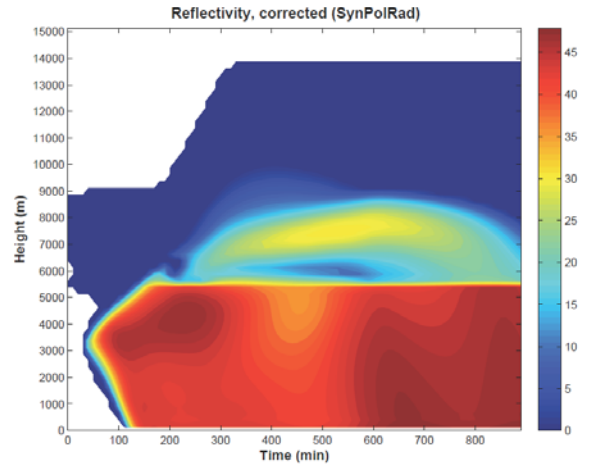

(b)

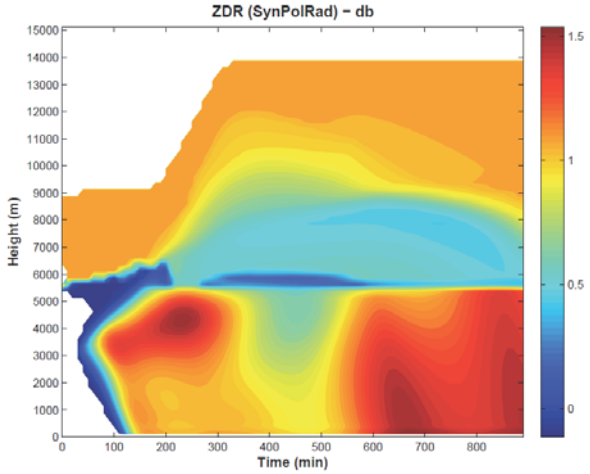

Figure 11: Reflectivity (a) and differential reflectivity (b) from simulated squall line by 1D lagrangian cloud model

For example, the differential reflectivity in Figure 11b shows sensitivity to particles at higher elevation, namely to the snow, which is not evident in the standard reflectivity measurement (Figure 11a). With the SymPolRad capability in the data assimilation system it would be possible to study impact of both types of information by the radar measurements with respect to optimizing bulk contribution of the microphysical processes in the model. So far the results simply demonstrate that our modeling system is working properly. We wish to point out that the SymPolRad software must be made more computationally efficient before it is used in MCMC experiments.

b) Analysis of contributions of different microphysical processes

In order to introduce new parameters in the model that would control contribution of different bulk cloud microphysical processes in the data assimilation experiments, the modeled time rate of change by each process and for each prognostic hydrometeor type must be identified in the model software. The identification of the processes in the model code is not trivial as the models are not typically designed for purpose of analysis of the time rate of change by individual processes. Van Lier-Walquie has performed initial "decomposition" of the microphysical scheme in the 1D-lagrangian model. The preliminary results are illustrated in Figure 12. This figure shows contributions of different processes to the time rate of change of the modeled rain. The rates are vertically integrated at each model time step. The results in Figure 12 show that dominant process for the rain production in the model is the accretion of cloud water by rain (red curve). This result is expected, especially during the convective phase (up to 400 time steps on the time axis). However, the peak values during the stratiform phase (after 500-th time step) seem high because they are of similar amplitude to the values during the convective phase, which is not expected. On the other hand, steady increase of melting of snow to rain is depicted realistically in the model during the stratiform phase, at least in terms of trend. The reality of actual magnitude of the melting time rate of change cannot be evaluated because it is not known. Regarding the depletion of rain, the dominant process in the model is accretion of rain by cloud ice, which peaks during the convective phase and is lagging in time after the peak in the rain production, as expected. The accretion of rain by snow is second largest sink. This sink peaks during transition between the convective and stratiform phases. The accretion of rain by snow is in phase with the production of rain by melting of snow, and they seem to nearly cancel each other until the accretion is exhausted by the peak of the stratifom phase.

We have performed the equivalent analysis of contributions of different processes for each other prognostic hydrometeor type in the model (not shown). We are currently evaluating accuracy of the data in these analyses in terms of making sure that the correct data are being extracted from the model simulation. As mentioned above, the model algorithm is not designed to evaluate time tendency terms that are produced by the individual microphysical processes. Consequently, special data output must be devised and tested for the purpose of our analysis.

Once the adequacy of data is confirmed, the results that are illustrated in Figure 12 and equivalent for the other hydrometeors would be used to define a set of control parameters in the data assimilation by MCMC with the radar reflectivity observations. In addition, the evolution of time rate of change by individual processes would be used as one of standard diagnostics when evaluating the impact of data assimilation to the modeling of the bulk microphysics.

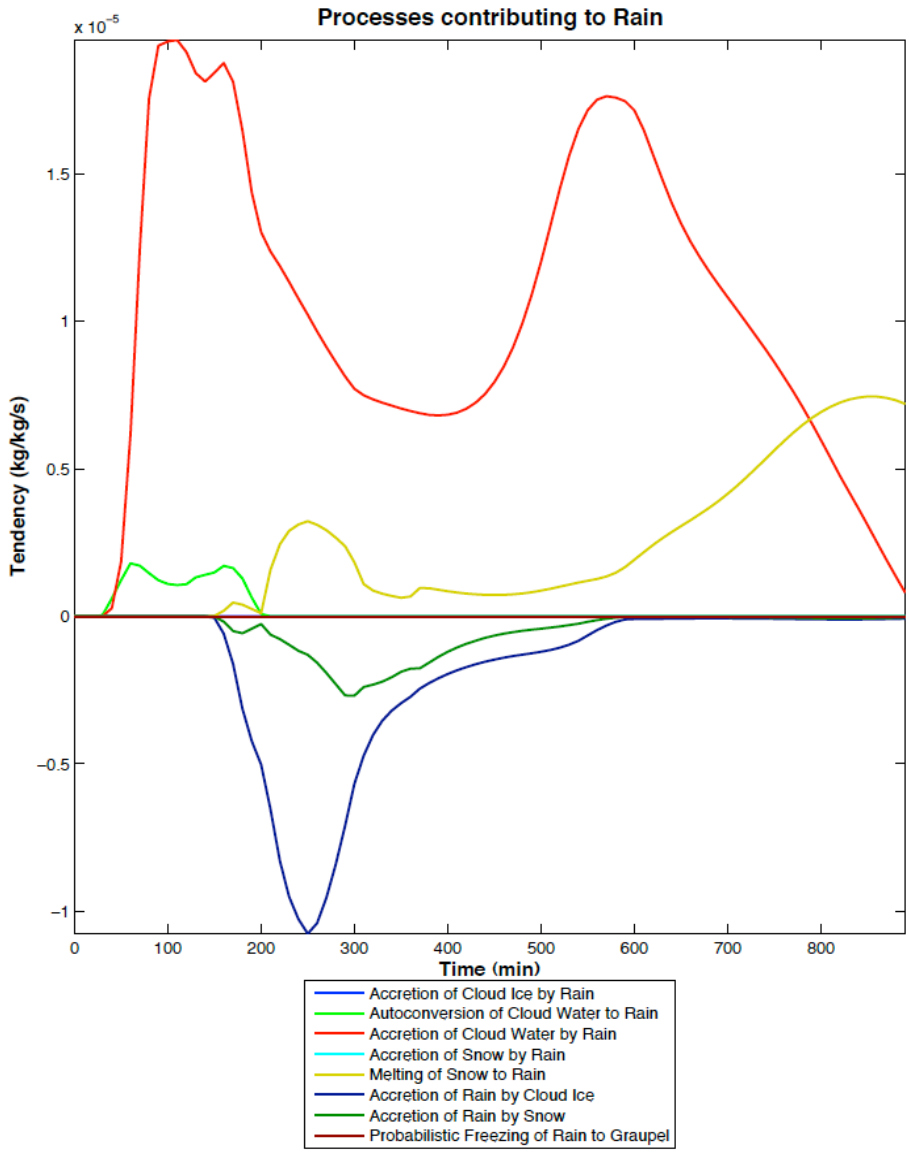

Major findings that were reported in the first report (March 2009)

Model verification and forming hypothesis about modeling errors

Model evaluation for the June 13 case by global diagnostics such as reflectivity histograms and 3D contingency tables in the radar reflectivity space indicate that the model forecast has extremely low skill relative to radar observations at point-by-point bases. For example, the 3D contingency tables in the binned reflectivities in Figure 1, for 3 different microphysical parameterizations, show that the model does not agree with the observations at more than 90% of the points in 3D domain only few hours into the forecast, despite almost perfect agreement at the initial time. The agreement at the initial time results from initialization with LAPS analysis which includes observed reflectivities. This initialization provides "hot start" to the forecast. The "hot start" initial model data include cloud and precipitation hydrometeor fields with adjusted wind, humidity and temperature fields.

In contrast to the point-vise diagnostics which show low forecast skill, comparison of 2D reflectivity horizontal cross-sections between the model and LAPS analysis indicates that the model captures some general features of the observed evolution of the storm system. For example, in the model and observations, the squall line which is present at the beginning of forecast for the June 13 case (0000 UTC) across Northern Texas, Western Oklahoma and South-East Kansas (shown in Figure 2) splits into two branches, denoted here SW (South-West) and NE (North-East). Both of the branches then persists over about 2 hours, moving in SE direction in the model and observations (illustrated in Figure 3). The movement of the storm front is somewhat faster in the model than in observations. Consecutive evolution, after 0200 UTC, includes dissipation of the SW branch both in the observations and model, but in the model there is secondary storm development ahead of the front, which is not present in the observations (Figure 4). Regarding the storm that is associated with the NE branch of the initial squall line, it intensifies and continues to move in S-SE direction in both the model and observations, but the observed is characterized with the squall line shape while modeled storm is not. The modeled storms also include much less area and weak secondary developments to the NE (Figure 4). These general features of the storm evolution are present in each model simulation with different microphysical parameterizations but intensity of storms and aerial coverage differ between the different schemes. For example, the Schultz scheme produces least aerial coverage and least skilled forecast. These results indicate that comparison of the modeled to observed reflectivity fields for the purpose of data assimilation with respect to the microphysical parameterizations should include only regions with equivalent coherent structures and only over the associated life time of few hours.

In addition to verification with the reflectivity data we compared 2D fields of temperature, horizontal wind and humidity between the forecast and LAPS analysis . This comparison indicates that the model has tendency to generate strong cold pool where there is storm activity in all regions and with all schemes, much stronger than the equivalent in the observationally-based analysis data. For example, the SW branch which dissipates entirely in the SW Oklahoma in the observations, intensifies in the model further south because the model generated cold pool interacts with warm environment forming strong convergence zone south of the storm and near the surface. This overcooling in the lower troposphere in the model forecast, that occurs from the onset with the initialized squall line, suggests that the cloud microphysical parameterizations control the forecast error by feedback with the dynamics. The overcooling in the model due to activated microphysical parameterizations early in the simulations in illustrated in Figure 5.

To better understand the model errors associated with the cooling due to the microphysics we plan to perform analysis of time tendency of temperature perturbations due to the parameterized

microphysical processes in the three schemes. For this purpose we need to generate additional model simulations to extract data that are not available in the standard output. In addition, because the LAPS analysis is relatively crude above the surface due to insufficient observation coverage, further identification of discrepancies between the model and reality regarding mesoscale interactions between the microphysical parameterization results and perturbations in temperature, humidity and wind within the regions of storm activity requires use of more observations. We are currently making selection of observations from the IHOP archive for this purpose.

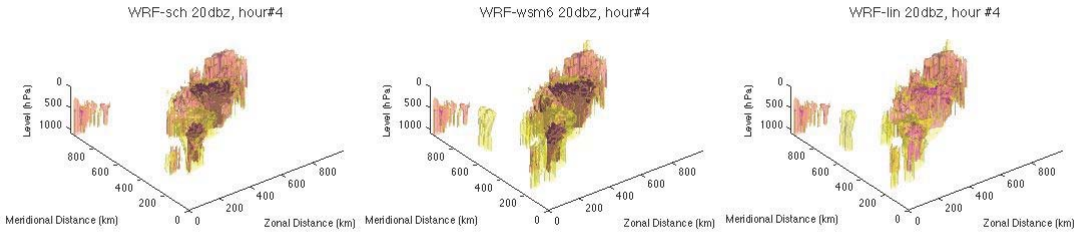

Figure 1: 3D contingency tables (model/observation "yes" or "no" occurrence in each spatial point) in radar reflectivity field for threshold of 20 dbz, for three model simulations using different cloud microphysics parameterizations at verification time 04 UTC June 13 2004 within model domain (model domain is depicted in next figures). White color indicates no/no (model/observation), black yes/yes, yellow (no/yes) and pink yes/no. Version of the precipitation microphysical parameterization is indicated in the panel title.

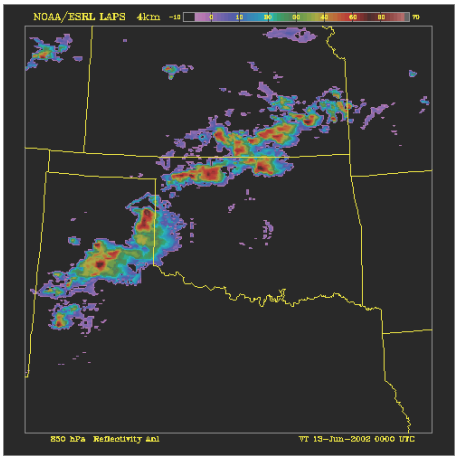

Figure 2: Observed reflectivity at 850 hPa level at initial time for June 13 case (0000 UTC, June 13, 2002).

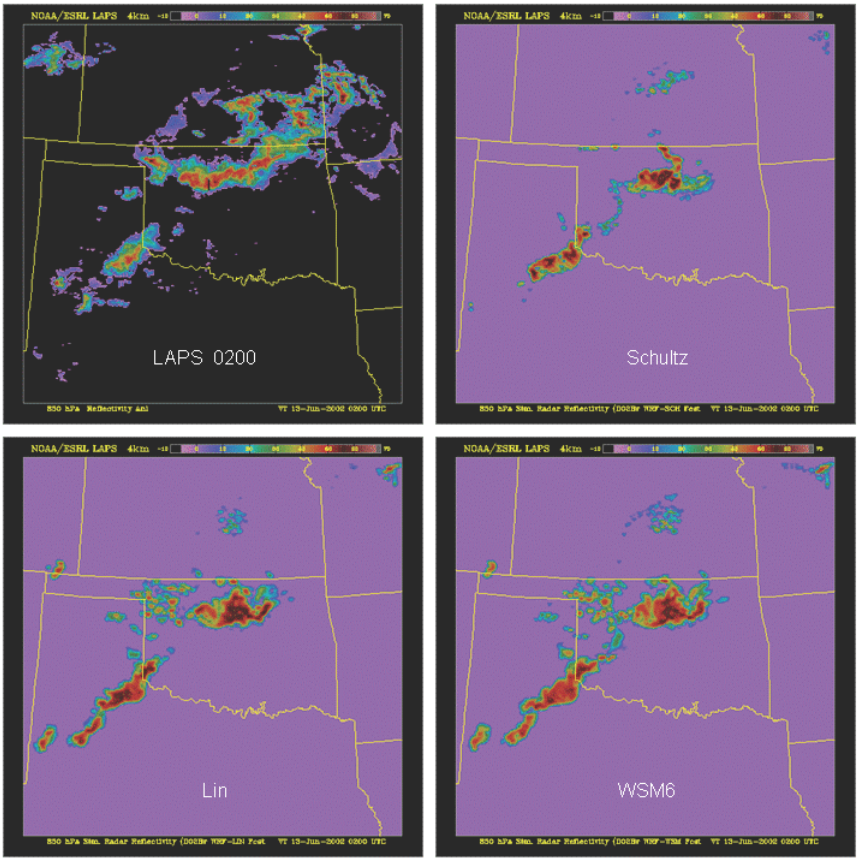

Figure 3: Observed and modeled reflectivity at 850 hPa level at 2 hours into the simulation (0200 UTC, June 13, 2002).

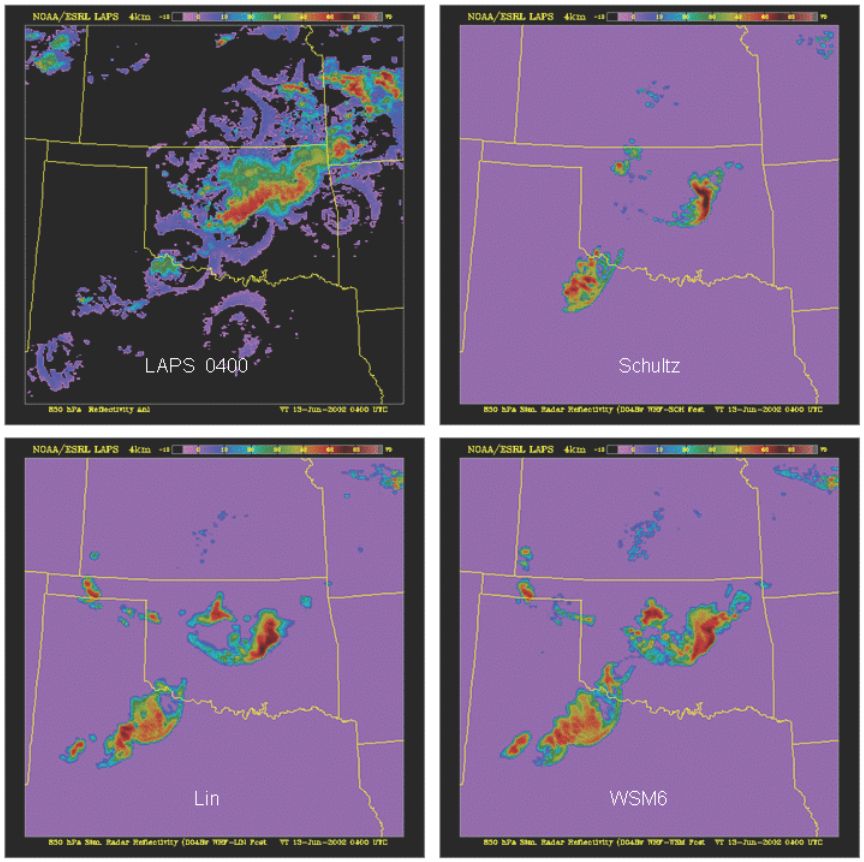

Figure 4: Observed and modeled reflectivity at 850 hPa level, at 4 hours into the simulation (0400 UTC, June 13, 2002).

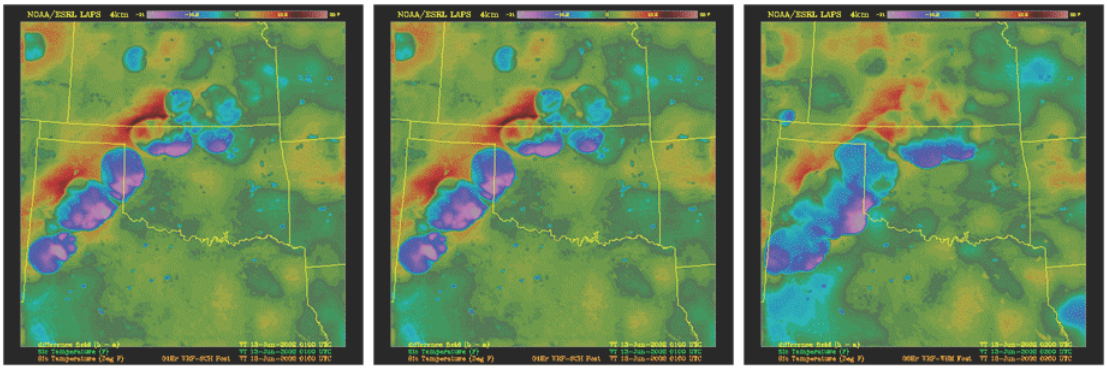

Figure 5: Differences in surface temperature between model simulations and LAPS analysis one hour into the simulations (0100 UTC, June 13, 2002). Cold colors are negative and near zero values are green. Maximum negative difference is about -15 C. Left panel is for WSM6, middle for Lin and right for Shultz microphysical parameterization.

References

Albers S., J. McGinley, D. Birkenheuer, and J. Smart 1996: The Local Analysis and Prediction System (LAPS): Analyses of clouds, precipitation, and temperature. /Weather and Forecasting /, *11*, 273-287.

Albers S. 1995: The LAPS wind analysis. /Weather and Forecasting/, *10*, 342-352.

Asai, T., 1965: A numerical study of the air-mass transformation over the Japan Sea in winter. *J. Meteorol. Soc. Jpn.,* **43,** 1-15.

Dudhia, J., 1989: Numerical study of convection observed during the winter monsoon experimentusing a mesoscale two-dimensional model, J. Atmos. Sci., 46, 3077–3107.

Hong, S.-Y., and J.-O. J. Lim, 2006: The WRF single-moment 6-class microphysics scheme (WSM6). J. Korean Meteor. Soc., 42, 2, 129-151.

Hong, S.-Y., H.-M. H. Juang, and Q. Zhao, 1998: Implementation of prognostic cloud scheme for a regional spectral model, Mon. Wea. Rev., 126, 2621–2639.

Lin, Y.-L., R. D. Farley, and H. D. Orville, 1983: Bulk scheme of the snow field in a cloud model. *J. Climate Appl. Meteor.,* **22**, 1065-1092.

McGinley, J.A. and J.R. Smart, 2001: On providing a cloud-balanced initial condition for diabatic initialization. /Preprints, 18th Conf. on Weather Analysis and Forecasting/, Ft. Lauderdale, FL, Amer. Meteor. Soc.

Michalakes, J., J. Dudhia, D. Gill, J. Klemp and W. Skamarock, 1998: Design of a next-generation regional weather research and forecast model : Towards Teracomputing, World Scientific, River Edge, New Jersey, 117-124.

Rutledge, S. A., and P. V. Hobbs, 1984: The mesoscale and microscale structure and organization of clouds and precipitation in midlatitude cyclones. XII: A diagnostic modeling study of precipitation development in narrow cold-frontal rainbands. *J. Atmos.Sci.,* **41,** 2949–2972.

Schultz, P. J., 1995: An explicit cloud parameterization for optional numerical weather prediction. *Mon. Wea. Rev*. **123**, 3331-3343.

Schultz, P. and S. Albers, 2001: The use of three-dimensional analyses of cloud attributes for diabatic initialization of mesoscale models. /Preprints, 14th Conf. on Numerical Weather Prediction/, Ft. Lauderdale, FL, Amer. Meteor. Soc.

Skamarock, W. C., J. B. Klemp, J. Dudhia, D. O. Gill, D. M. Barker, W. Wang and J. G. Powers, 2005: A Description of the Advanced Research WRF Version 2, NCAR technical note.

Tao, W.-K., J. Simpson, and M. McCumber 1989: An ice-water saturation adjustment, Mon. Wea. Rev., 117, 231–235.

Troen, I., and L. Mahrt, 1986: A simple model of the atmospheric boundary layer: Sensitivity to surface evaporation. Bound.-Layer Meteor., 47, 129-148.